Lasers in Surgery and Medicine 19:23–31 (1996)

Time-Resolved Observations of Shock Waves and Cavitation Bubbles Generated by Femtosecond Laser Pulses in Corneal Tissue and Water

Tibor Juhasz, PhD, George A. Kastis, BS, Carlos Suárez, MS, Zsolt Bor, PhD, and Walter E. Bron, PhD

Department of Physics, University of California, Irvine (T.J., G.A.K., C.S., Z.B., W.E.B.); Intelligent Surgical Lasers, San Diego, California 92121 (T.J.); Department of Optics and Quantum Electronics, JATE University, Dom ter 9, Hungary (Z.B.)

Background and Objective: **Photodisruption in ocular media with high power pulsed lasers working at non-absorbing frequencies have become a well established surgical tool since the late seventies. Shock waves and cavitation bubbles generated by the optical breakdown may strongly influence the surgical effect of photodisruptive lasers. We have investigated the shock wave and cavitation bubble effects of femtosecond laser pulses generated during photodisruption in corneal tissue and water. The results are compared to those obtained with longer laser pulses.**
Study Design/Materials and Methods: **Laser pulses with 150 fs duration at ~620 nm wavelength have been focused into corneal tissue and water to create optical breakdown. Time-resolved flash photography has been used to investigate the dynamics of the generated shock waves and cavitation bubbles.**
Results: **A rapid decay of the shock waves is observed in both materials with similar temporal characteristics and with a spatial range considerably smaller than that of shock waves induced by picosecond (or nanosecond) optical breakdown. Cavitation bubbles are observed to develop more rapidly and to reach smaller maximum diameter than those generated by longer pulses. In corneal tissue, single intrastromal cavitation bubbles generated by femtosecond pulses disappear within a few tens of seconds, notably faster than cavitation bubbles generated by picosecond pulses.**
Conclusions: **The reduced shock wave and cavitation bubble effects of the femtosecond laser result in more localized tissue damage. Therefore, a more confined surgical effect should be expected from a femtosecond laser than that from picosecond (or nanosecond) lasers. This indicates a potential benefit from the applications of femtosecond laser technology to intraocular microsurgery.** © 1996 Wiley-Liss, Inc.

Key words: laser-tissue interactions, laser-generated shock waves and cavitation bubbles in cornea and water, femtosecond lasers, time-resolved flash photography, intraocular surgery, intrastromal photorefractive keratectomy

INTRODUCTION

Photodisruption in ocular media generated with high power pulsed lasers operating at non-absorbing frequencies (at least to first order) has

Accepted for publication March 20, 1995.

Address reprint requests to Tibor Juhasz, Department of Physics, University of California, Irvine, CA 92717.

become a well-established tool for intraocular microsurgery since the 1970s [1–3]. Damage from a photodisruptive laser is initiated by optical breakdown at the focus of the laser beam, and the plasma created in this way initially expands with hypersonic velocity as a result of the plasma pressure and temperature [4]. A shock wave is emitted when the plasma expansion decreases to subsonic velocity [5]. Further expansion of the plasma results in the creation of a cavitation bubble [6–11], followed by the implosion of the cavitation bubble, which may create secondary acoustic transients, such as radially propagating acoustic waves [12]. There are indications that the primary surgical effect of the photodisruptive lasers is due to tissue evaporation by the laser plasma [8–11,13]. Shock waves and cavitation bubbles may cause extended collateral tissue damage if they reach large magnitudes. In the case of nanosecond pulses, with energies in the millijoule range, collateral tissue damage has been observed in a large volume due to acoustic side effects [8,9]. A strong reduction of the collateral tissue damage has been achieved with picosecond pulses of energies typically in the range of a few tens of microjoules [8–11,13].

Recent developments in laser technology have demonstrated that stable generation of femtosecond laser pulses is possible with solid-state lasers. The availability of stable amplified femtosecond laser pulses suggests, on the one hand, their applications to intraocular surgery and, on the other hand, generates questions of the possible advantage compared to already existing laser surgical techniques. As previous experiments have indicated, the threshold energy for optical breakdown is proportional to the square root of the duration of the laser pulse in ocular media [13,14]. Therefore, optical breakdown can be achieved with even smaller energies with femtosecond laser pulses. This indicates that shock wave and cavitation bubble effects and heat transfer to the tissue may be further reduced if femtosecond laser technology is used during intraocular surgery.

To verify the possible benefit that femtosecond lasers bring to intraocular surgery and to evaluate the application of femtosecond lasers in comparison to the techniques currently in use, we have investigated the shock wave emission and cavitation bubble formation after femtosecond optical breakdown in cornea and in water using a time-resolved flash photography technique.

MATERIALS AND METHODS

Experimental Apparatus

A laser system generating amplified femtosecond and picosecond laser pulses simultaneously at different wavelengths is used to perform the experiments [15]. The femtosecond pulses are used to create optical breakdown in the samples, whereas the picosecond pulses provide the flash for the time-resolved photography. The experimental arrangement is outlined in Figure 1. The system begins with a cw-pumped, actively modelocked, Nd:YAG master oscillator, which delivers pulses of ~100 ps duration at 1.064 μm wavelength at a 76 MHz repetition rate. After frequency doubling in a KTP crystal, 1 W of 532 nm radiation is obtained, which is used to synchronously to pump a linear cavity femtosecond dye laser [15]. The standard six-mirror linear cavity femtosecond dye laser is equipped with intracavity group velocity dispersion control and delivers pulses of ~130 fs duration at ~620 nm wavelength with an average power of ~50 mW. The output of the femtosecond dye laser is synchronously amplified through a two-stage dye amplifier chain using quartz cuvettes with flowing dyes of Kiton Red at a concentration of $\sim 10^{-4}$ moles in water. A Nd:YAG regenerative amplifier is seeded with a small portion of the IR output of the master oscillator. The frequency doubled output of the regenerative amplifier is then used to pump the dye amplifier chain. In order to suppress the amplified spontaneous emission and the unamplified background, a saturable absorber dye jet is placed between the two amplifier stages. After amplification, the pulse energy and the pulse duration are measured to be ~3 μJ and ~150 fs, respectively. The repetition rate of the amplified pulses can be varied between 25 Hz and 1 kHz. The amplified femtosecond pulses are transmitted through a variable density optical filter for fine adjustment of the energy before they are applied to the samples.

In order to provide the synchronized flash pulses used for the time-resolved photography, pulses from the output of the master oscillator are amplified in a second regenerative amplifier. A second harmonic generator unit is used to convert the amplified near-infrared laser pulses into visible light at 532 nm wavelength. The duration of the green pulses is measured to be ~60 ps, which determines the time resolution of the system. The relative timing between the two regenerative amplifiers is adjusted by steps corresponding to the

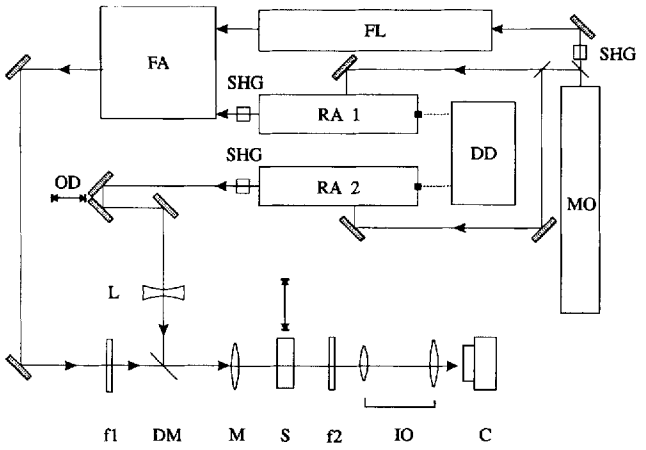

Fig. 1. The schematic diagram of the experimental apparatus. MO, Nd:YAG master oscillator; SHG's, second harmonic generator crystals, FL, linear cavity synchronously pumped femtosecond dye laser; RAs, Nd:YAG regenerative amplifiers; DD, digital delay generator; FA, synchronously pumped femtosecond dye amplifiers; OD, variable optical delay; L, lens (f = −30 cm); F1 variable density filter; DM, dichroic mirror; M, microscope objective (magnification: 16×); S, sample; F2, interference filter; IO, imaging optics; C, CCD camera.

time interval between two oscillator pulses (13 ns) by means of a digital delay generator. A fine adjustment of the time delay below 13 ns is provided by a variable optical delay.

Bovine corneas are used in our study. The eyes had been enucleated several hours prior to the experiments. The corneas were removed a few minutes before the laser illumination and placed between two glass plates, which prevented the loss of water during the experiments. An outline of the photographic apparatus is displayed in Figure 1. The femtosecond surgical beam is at near normal incidence to the corneal surface and is focused to a diameter of ~5 μm in the cornea. Measurements of the spot size have been carried out with a knife edge. A divergent illumination beam is directed to the same beam pass as the surgical beam with a dichroic mirror and is focused into the cornea with the same objective. Due to its divergence, the focal plane of the illumination beam is behind that of the surgical beam. Therefore the green beam illuminates the focal spot of the surgical pulse and its surrounding area. An interference filter blocks out the surgical beam behind the sample and the green beam is imaged to a CCD camera (ELMO model MN401E) with the help of two microscope objectives. The picture provided by the CCD camera is recorded by a video recorder. The spatial resolution of the imaging system is estimated to be ~2 μm. In order to ensure recording single events in each video frame with our simple nongated camera, electronically triggered shutters select single pulses from the surgical and illumination beams.

The cornea is replaced with a rectangular glass cuvette for comparative studies in water. Repetitive measurements were taken since both the shock wave and cavitation are completely relaxed in water by the time the next surgical laser pulse arrives at the target. Contrary to this, the laser pulses introduce irreversible changes in tissue. Therefore the corneal samples are moved across the laser beams by a stepper motor to ensure that each pulse interacts with undamaged tissue.

RESULTS

We first determined the threshold fluence of the optical breakdown inside the cornea and in tap water. Since the fluorescent light of the femtosecond optical breakdown is rather weak at intensities around the threshold, we used the appearance of the cavitation bubbles as an indication of optical breakdown. In order to complete the measurements, the fluence of the surgical laser pulse is slowly increased from below threshold level until the appearance of the cavitation bubbles is observed with the high resolution imaging apparatus. The disappearance of cavitation bubble generation is observed with decreasing pulse energy. The threshold fluences in cornea and in tap water are 1.3 J/cm^2 and 0.87 J/cm^2, respectively, as calculated from the measurements of the pulse energy and the spot size. The threshold fluence in the stroma is only slightly higher than that measured on the corneal surface [13]. As compared to other threshold measurements with longer pulses [5,13,14,16], both measurements support earlier observations that the optical breakdown threshold is proportional to the square root of the pulse duration.

The dynamics of the shock waves are investigated with a series of pictures taken with increasing time delay between the optical breakdown and the exposure of the picture. Photographs of shock waves obtained in bovine cornea and water are shown a and b, respectively, in Figure 2. The density of the material, and therefore the optical refraction, is changed in the shock wave front, which deflects some light out from the aperture of the imaging lens system. Thus the shock wave appears as a dark ring in the pictures.

The distance of the shock front from its cen-

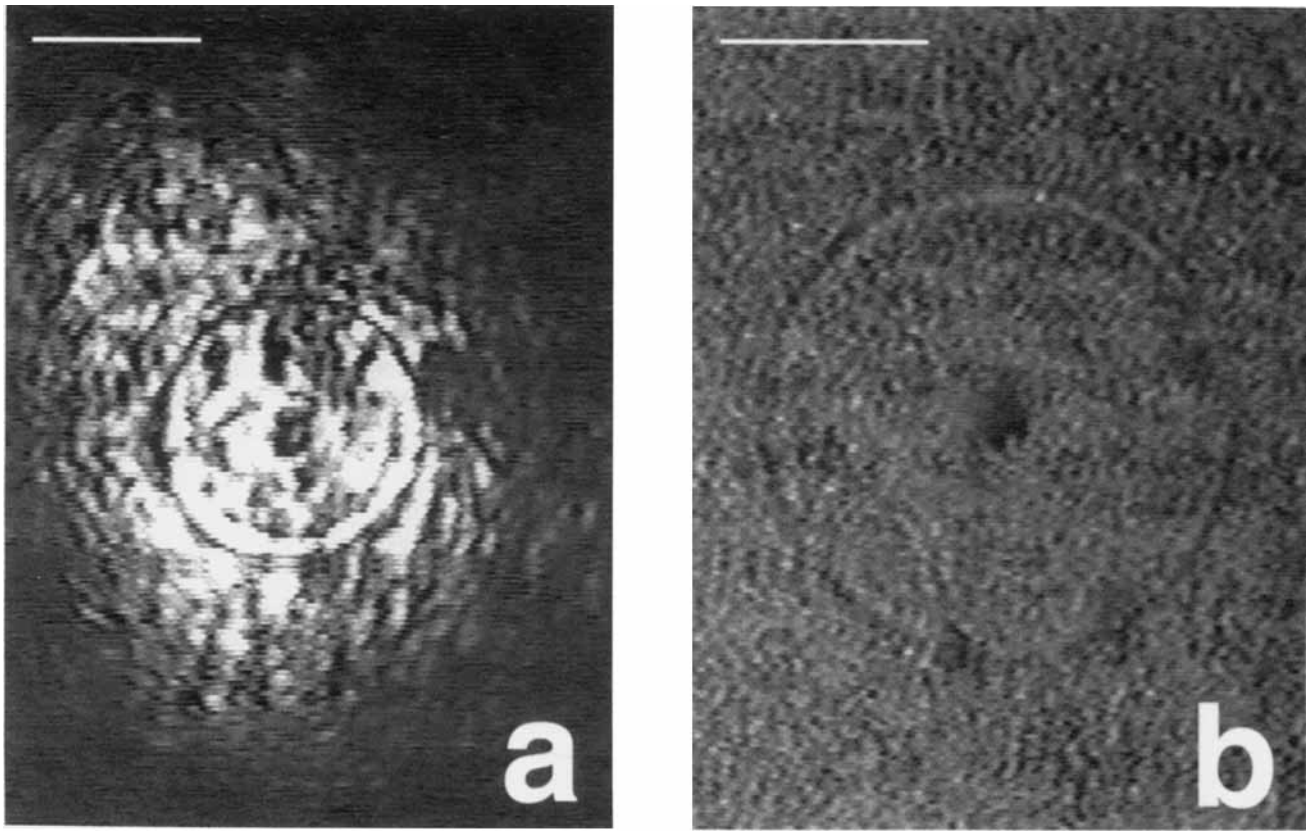

Fig. 2. Shock waves photographed 8 ns after the optical breakdown in bovine cornea (**a**), and 12.8 ns after the optical breakdown in water (**b**). The laser fluences are 15 J/cm^2 and 9 J/cm^2, respectively. Bar = 20 μm.

ter, defined as the radius of the shock wave, is measured in directions perpendicular to the propagation direction of the light. Figure 3 displays the shock wave radius as a function of time. The displayed data are taken in bovine cornea samples (open circles) and in water (filled circles) with laser fluences 15 J/cm^2 and 9 J/cm^2, respectively. Each data point is an average of 8–10 measurements obtained in separate events. The error bars are the standard deviations. The sizes of the error bars are ~2 μm, which is consistent with the spatial resolution of the system. (The error bars are not visible in Fig. 3 since their sizes are slightly smaller than those of the symbols.) Nonlinear time dependence of the shock wave radius is observed only in the first ~10 ns after the optical breakdown indicating the rapid decay of the shock wave. The solid line represents a linear fit to the data obtained in water with delays longer than ~10 ns.

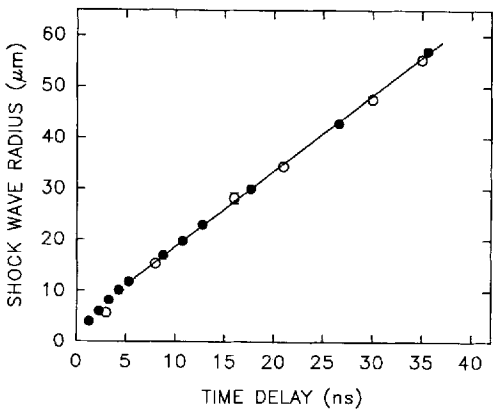

Fig. 3. The shock wave radius as a function of time in bovine cornea (open circles), and in water (filled circles). The laser fluences are 15 J/cm^2 and 9 J/cm^2, respectively. The solid line is a linear fit to the data obtained in water ~10 ns after the impact of the laser. The velocity of the sound in water is measured to be v_s = 1,488 m/s from the slope of the line.

The velocity of the shock wave as a function of the shock wave radius is shown in Figure 4. The open circles represent results obtained in cornea samples, and the filled circles display results in water. The shock wave velocity is obtained by a simple numerical differentiation with respect to

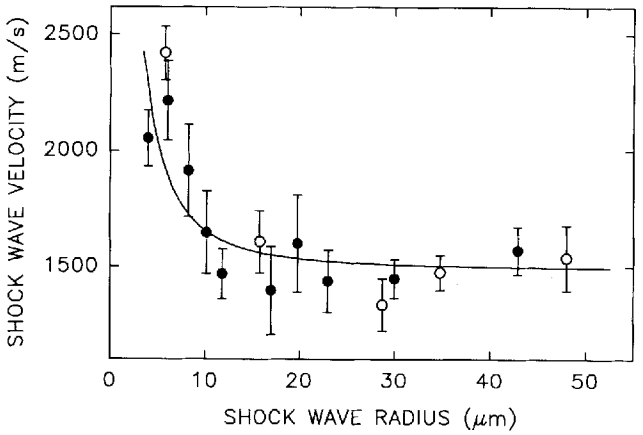

Fig. 4. The shock wave velocity as a function of the shock wave radius in bovine cornea (open circles) and in water (filled circles) as calculated from the data displayed in Figure 3. The solid line represents the one parameter fit of Eq. 1 to the data obtained in water.

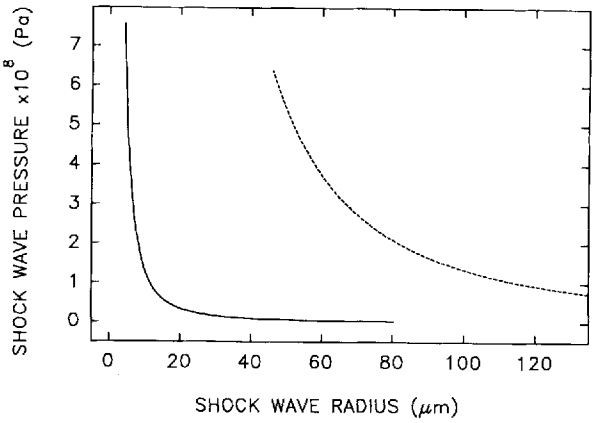

Fig. 5. The shock wave pressure as a function of the shock wave radius in water generated by laser pulses with fluences of 9 J/cm^2. (1Pa = 1N/m^2 = 10^{-5} bar)

the time of the data displayed in Figure 3. The differentiation is defined as $\Delta r/\Delta t = (r_{i+1} - r_i)/(t_{i+1} - t_i)$ where r_i is the radius of the shock wave at time t_i. The procedure starts at the first measured value of r_i. The above derivation of the shock wave velocity results in a superposition of the experimental uncertainties of r_{i+1} and r_i, which is indicated by the increased sizes of the error bars in Figure 4.

As the high velocity shock wave propagates through the medium, it loses energy and decays to a harmless acoustic wave that propagates with the velocity of the sound. The velocity of sound in water, as is determined from the slope of the line fit in Figure 3, is found to be 1,488 m/s. The velocity of sound in cornea is found to be 1,463 m/s using the same method. The dissipation of the shock waves takes place within ~10 ns in both media, corresponding to a radius of ~20 μm. The above observations indicate that the dynamics of the shock waves generated by femtosecond optical breakdown is similar in corneal tissue and in water. This confirms previous results obtained with picosecond pulses [12].

We focus our further analysis of shock wave dynamics on water since the parameters of this material are well known. Following the analysis of ref. [17], we determine the shock wave pressure generated by the femtosecond laser pulses. First, we fit the theoretical function

$$v_s(r) = \frac{A}{2} + \sqrt{\frac{A^2}{4} + \frac{C}{r^2}} \qquad (1)$$

which describes the velocity of the shock wave as a function of radius to the measured values of shock wave velocities. Here r is the radius of the shock wave, $v_s(r)$ is the shock wave velocity, A = 1,488 m/s (velocity of sound in water), and C is a fitting parameter. The value C is obtained to be 2.7×10^{-5} m^4/s^2 at the best fit, which is shown as a solid line in Figure 4. The shock wave pressure is determined from the expression

$$P(r) = C \frac{\rho_o}{B} \frac{1}{r^2} \qquad (2)$$

where P(r) represents the shock wave pressure as a function of the shock wave radius, C is the fitting parameter obtained from the velocity curve, ρ_o = 998 kg/m^3 is the density of water [18], and B = 2.07 [19]. The above values of A and B are valid for pressure values up to 2×10^9 Pa (20 kbar). A higher order approximation for calculating P(r) is given in ref. [20]. The shock wave pressure as a function of the shock wave radius is displayed by the solid curve in Figure 5. The pressure at the closest observable point to the optical breakdown was ~8×10^8 Pa (8 kbar). The shock wave pressure approaches zero within a radius of ~20 μm away from the optical breakdown.

The increase of the delay time to the submicrosecond and microsecond range made it possible to observe the temporal evolution of the cavitation bubbles. Figure 6a,b displays examples of cavitation bubbles in cornea and water, respectively. The diameter of the cavitation bubbles generated by the femtosecond optical breakdown as a function of time is shown in Figures 6 and 7

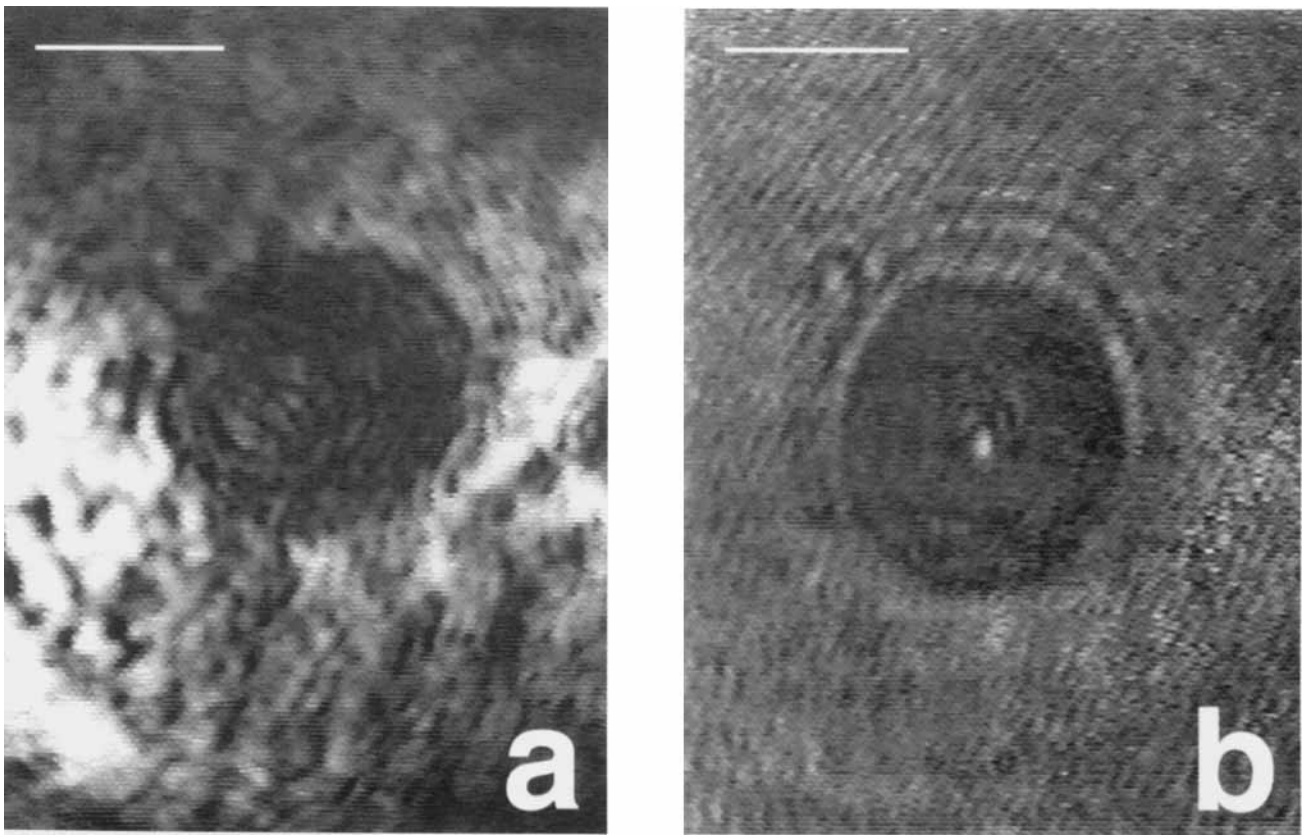

Fig. 6. Cavitation bubbles photographed 1 μs after the optical breakdown in bovine cornea (**a**) and 6 μs after the optical breakdown in water (**b**). The laser fluences are 16 J/cm^2 and 9 J/cm^2, respectively. Bar = 20 μm.

in bovine cornea and water, respectively. Laser fluences of 15 J/cm^2 in cornea and 9 J/cm^2 in water are applied. Measurements are taken in steps of 10 ns for the first 100 ns, and in steps of 100 ns afterward. For each delay, time measurements from 8–10 independent events are averaged. The error bars represent the standard deviations. As can be seen in Figures 6 and 7, the cavitation bubbles reach their maximum size within 650 ns in corneal tissue and within 2.7 μs in water. The maximum bubble radius is ~23 μm in the corneal tissue and ~27 μm in water. In cornea a small bubble remains in the tissue after one oscillation that possess a period time of ~5 μs. The small bubble disappears within 15–30 seconds. The increased size of error bars in the case of water is due to the increased fluctuations of the bubble size observed during the collapsing phase.

We now turn to the comparison of the measured values of the bubble radius in water to theory. Rayleigh [21] has derived the maximum diameter of the cavitation bubbles, R_{max}, as

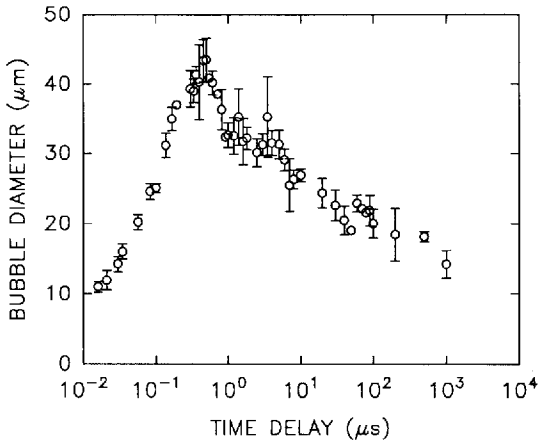

Fig. 7. The diameter of the cavitation bubbles in bovine cornea as a function of time shown in a semilogarithmic plot. The laser fluence is 15 J/cm^2.

$$R_{max} = \frac{T_c}{0.915\sqrt{\frac{\rho_o}{p_o - p_v}}} \qquad (3)$$

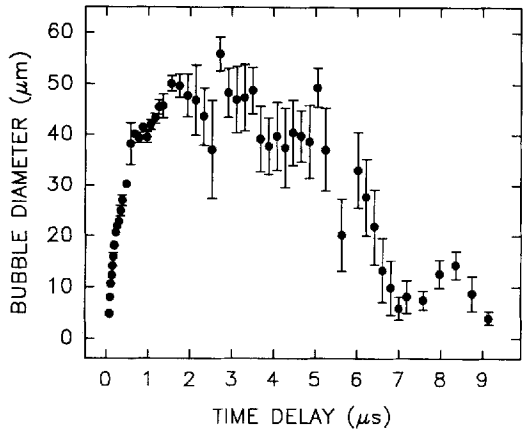

Fig. 8. The diameter of the cavitation bubble in water as a function of time. The laser fluence is 9 J/cm^2.

where ρ_o denotes the density of water (ρ_o = 998 kg/m^3), p_o is the pressure in the water at the bubble wall, p_v is the vapor pressure, and T_c denotes the collapse time for the bubble. The values of p_o and p_v are determined in ref. [18] to be 101.5 kPa and 2.6 kPa, respectively. The above equation assumes a spherical bubble, in which the time of collapse is equal to the time of growth [22]. We measured the time of growth to be ~ T_c = 2.7 μs. Using this value to calculate the maximum of cavitation bubble radius with Rayleigh's equation, we obtain R_{max} = 29 μm. This is within reasonable agreement with the measured value of $R_{max} \approx$ 27 μm.

DISCUSSION

It is important to compare our data to previously obtained results on the dynamics of shock waves and cavitation bubbles generated with picosecond laser pulses. In order to compare the results on shock waves, we plot the pressure of shock waves generated by femtosecond and picosecond optical breakdown as a function of the shock wave radius in Figure 5 with solid and dashed curves, respectively. The picosecond data are copied from Figure 5 of ref. [12]. Both the femtosecond and the picosecond data were obtained with laser fluences approximately ten times above the threshold. Figure 5 indicates a considerably faster decay of the shock waves generated by femtosecond optical breakdown. To make this comparison more quantitative, we assume isotropic propagation of the shock wave and arbitrarily define the range of shock wave at a distance when its pressure decreases below 3 × 10^7 Pa. (At low pressure values the accuracy of our method, to determine the shock wave pressure, is limited [17].) We estimate the volume of tissue effected by the shock wave by calculating the volume of a sphere with a radius equal to the range of the shock wave. We obtain V = 4 × 10^{-5} mm^3 for femtosecond and V = 4 × 10^{-2} mm^3 for picosecond optical breakdown. This indicates that the volume of the tissue effected by the shock wave is ~1,000 times less if femtosecond, rather than picosecond, laser pulses are used during surgery. Obviously, an even more drastic reduction of the shock wave is observed if the current results are compared to traditional nanosecond photodisruptive lasers, e.g., a Nd:YAG laser.

Similarly to the range of the shock wave, the size of the cavitation bubbles is also considerably reduced if picosecond photodisruptive lasers are replaced with femtosecond ones. In corneal tissue the diameter of the cavitation bubbles, measured 1 ms after the impact of the laser, is ~14 μm (see Fig. 7) contrary to the ~80 μm diameter of the bubbles generated by picosecond pulses [12]. In both cases fluences exceeding the threshold by ~10 times are used in the experiments. Similar reduction in the maximum diameter of the cavitation bubbles is observed in corneal tissue as well as in water. A faster development and collapse of the bubbles generated with femtosecond pulses is observed, which is consistent with their smaller diameter. Furthermore, full disappearance of the bubbles in corneal tissue occurs within 15–30 seconds, contrary to 10–30 minutes observed in the case of picosecond laser-induced cavitation bubbles [12].

Side effects, especially cavitation bubbles, play an important role in intrastromal refractive surgery. In a procedure called intrastromal photorefractive keratectomy (ISPRK), also frequently referred to as "intrastromal ablation," a series of ultrashort laser pulses are used to destroy tissue inside the corneal stroma in order to alter the refractive power of the eye. The procedure shows initial success to correct myopia in animal experiments [23]. As is suggested by previous results [8–11,13], tissue removal is due to the effect of the laser plasma. It follows that the most efficient tissue removal can be achieved by placing the approximately spherical shaped micro-plasmas adjacent to each other. If the cavitation bubble generated by the first laser pulse is larger than the actual plasma size, it may interact with the surgical effect of the next pulse. Moreover if the impact of the pulse occurs inside

an existing cavitation, it does not remove tissue but increases the size of the cavitation through heat transfer to the gas. In order to avoid reheating the gas inside the cavitation, the next pulse must impact the tissue outside the bubble. Therefore, in the optimum case, the ratio of the cavitation diameter at the moment of the arrival of the next pulse, D_c, and the plasma diameter, D_p, should approach unity. (D_c is measured after the transient oscillations at the commonly used 1 kHz or lower repetition rates.) Using the data obtained with femtosecond laser pulses and the picosecond data previously published in ref. [12] allows us to determine D_c/D_p for both cases. In the case of femtosecond optical breakdown, we obtain $D_c/D_p \approx 3$; for picosecond optical breakdown, $D_c/D_p \approx 4$. Laser fluences approximately ten times above the threshold were used in both cases. Although in the high laser fluence range, this result is in good agreement with the empirical relation that $D_c \propto E^{1/3}$ [12], where E is the energy of the laser pulse, further investigations are necessary for laser fluences close to the threshold where $D_c \propto E$ [12], for which a larger difference is expected between the D_c/D_p ratios. These results suggest that the efficiency of ISPRK may be increased if femtosecond laser pulses are used.

CONCLUSIONS

The dynamics of shock waves and cavitation bubbles generated by femtosecond optical breakdown have been investigated in corneal tissue and water with time-resolved flash photography. The experimental results have shown that the use of femtosecond laser pulses for photodisruption results in a strong reduction in the magnitude of acoustic side effects such as shock waves and cavitation bubbles. Therefore the surgical effect of femtosecond laser pulses is more localized than that of picosecond (or nanosecond) pulses. This indicates the potential of femtosecond laser technology for applications in high precision intraocular microsurgery.

ACKNOWLEDGMENTS

The authors thank Intelligent Surgical Lasers for providing the CCD camera and a Nd:YAG regenerative amplifier. This research was supported through US-Hungarian Science and Technology Fund 06/90, and funds from NSF DMR931175 and ARO DAAHO 93-G-0188. G. A. K. received support from the UCI Honor Student Program.

REFERENCES

1. Steinert RF, Puliafito CA. The Nd:YAG laser in ophthalmology. Philadelphia: W.B. Saunders, 1985.
2. Krasnov MM. Laser puncture of anterior chamber angle in glaucoma. Am J Ophthalmol 1973; 75:674–678.
3. Frankhauser F, Roussel P, Steffen J, van der Zypen E, Chernakova A. Clinical studies on the efficiency of high power laser radiation upon some structures of the anterior segment of the eye. Int Ophthalmol 1980; 3:129–139.
4. Barness PA, Rieckhoff KE. Laser induced underwater sparks. Appl Phys Lett 1968; 13:282–284.
5. B. Zysset B, Fujimoto JG, Deutsch TF. Time resolved measurements of picosecond optical breakdown. Appl Phys B 1989; 48:139–147.
6. Fujimoto JG, Lin WZ, Ippen EP, Puliafito CA, Steinert RF. Time-resolved studies of Nd:YAG laser-induced breakdown. Invest Ophthalmol Vis Sci 1985; 26:1771–1777.
7. Vogel A, Hentschel W, Holzfuss J, Lauterborn W. Cavitation bubble dynamics and acoustic transient generation in ocular surgery with pulsed neodymium:YAG laser. Ophthalmol. 1986; 93:1259–1269.
8. Zysset B, Fujimoto JG, Puliafito CA, Birngruber R, Deutsch TF. Picosecond optical breakdown: Tissue effects and reduction of collateral damage. Lasers Surg Med 1989; 9:193–204.
9. Vogel A, Schweiger P, Freiser A, Asyo MN, Birngruber R. Intraocular Nd:YAG laser surgery: Light-tissue interactions, damage range, and reduction of collateral effects. IEEE J Quant Electron 1990; 26:2240–2260.
10. Vogel A, Busch S, Jungnickel K, Birngruber R. Mechanism of intraocular photodisruption with picosecond and nanosecond laser pulses. Lasers Surg Med 1994; 15:32–43.
11. Vogel A, Capon MR, Asyo-Vogel MN, Birngruber R. Intraocular photodisruption with picosecond and nanosecond laser pulses: Tissue effects in cornea, lens, and retina. Invest Ophthalmol Vis Sci 1994; 35:3022–3044.
12. Juhasz T, Hu, XH, Turi, L, Bor Z. Dynamics of shock waves and cavitations generated by picosecond laser pulses in corneal tissue and water. Lasers Surg Med 1994; 15:91–98.
13. Niemz M.H, Hoppeler T, Juhasz T, Bille JF. Intrastromal ablations for refractive corneal surgery using picosecond infrared laser pulses. Lasers Light Ophthalmol 1993; 5:145–152.
14. Stern D, Schoenline RW, Puliafito CA, Dobi ET, Birngruber R, Fujimoto JG. Corneal ablation by nanosecond, picosecond, and femtosecond lasers. Arch Ophthalmol 1989; 107:587–592.
15. Juhasz T, Smith GO, Mehta SM, Harris K, Bron WE. Generation and kilohertz rate amplification of synchronized femtosecond and picosecond laser pulses. IEEE J Quant Electron 1989; 25:1704–1707.
16. Du D, Squier J, Kurtz R, Elner V, Liu X, Gutmann G, Mourou G. Damage threshold as a function of pulse duration in biological tissue. In Barbara PF et al., eds. "Ultrafast Phenomena IX." New York: Springer, 1995, pp 254–255.

17. Doukas AG, Zweig AD, Frisoli JK, Birngruber R, Deutsch TF. Non-invasive determination of shock wave pressure generated by optical breakdown. Appl Phys B 1991; 237–245.
18. Ward B, Emmony DC. Interferometric studies of the pressures developed in a liquid during infrared-laser-induced cavitation-bubble oscillation. Infrared Phys 1991; 32: 489–515.
19. Harris P, Presles NH. Reflectivity of a 5.8 kbar shock front in water. J Chem Phys 1981; 74:6864–6866.
20. Rice MH, Walsh JM. Equation of state of water to 250 kilobars. J. Chem Phys 1957; 26:824–830.
21. Rayleigh GE. On the pressure developed in a liquid during the collapse of a spherical cavity. Phil Mag 1917; 34:94–98.
22. Lauterborn W. Laser-induced cavitation. Acustica 1974; 31:51–78.
23. Habib MS, Speaker MG, Kaiser R, Juhasz T. Myopic intrastromal photorefractive keratectomy with the Nd:YLF picosecond laser in the cat cornea. Arch Ophthalmol. 1995; 113:499–503.